

Catalysis Science & Technology

Accepted Manuscript



This is an *Accepted Manuscript*, which has been through the Royal Society of Chemistry peer review process and has been accepted for publication.

Accepted Manuscripts are published online shortly after acceptance, before technical editing, formatting and proof reading. Using this free service, authors can make their results available to the community, in citable form, before we publish the edited article. We will replace this *Accepted Manuscript* with the edited and formatted *Advance Article* as soon as it is available.

You can find more information about *Accepted Manuscripts* in the [Information for Authors](#).

Please note that technical editing may introduce minor changes to the text and/or graphics, which may alter content. The journal's standard [Terms & Conditions](#) and the [Ethical guidelines](#) still apply. In no event shall the Royal Society of Chemistry be held responsible for any errors or omissions in this *Accepted Manuscript* or any consequences arising from the use of any information it contains.



Journal Name

ARTICLE

Preparation and catalytic behavior of biomorphic calcium oxide/carbon solid base materials

Lan Wang, Changmiao Di, Ting Li, Yuan Chun*, Qinhua Xu

Received 00th January 20xx,
Accepted 00th January 20xx

DOI: 10.1039/x0xx00000x

www.rsc.org/

Using plant materials as templates is a convenient and low-cost route to prepare solid base catalysts with high specific surface area. In this study, a series of biomorphic calcium oxide/carbon catalysts have been prepared via *in situ* transformation technique using rice grains as a template and carbon precursor. The resulting CaO/carbon materials are spindly shaped catalyst and show high specific surface area and strong basicity. In the methylation of cyclopentadiene, these CaO/carbon materials exhibit higher catalytic performance than MgO/carbon materials and CaO prepared by directly calcining CaO precursor. Moreover, the regeneration of deactivated catalyst is studied, and the steam or CO₂ treatment at high temperature is found very effective for this carbon supported catalyst, and can even promote the catalytic activity. A possible mechanism for the deactivation and regeneration of the CaO/carbon materials has been proposed.

Introduction

The gasoline with high quality is extremely demanded with the development of transportation vehicles manufacturing and stricter regulations on environmental protection. The leaded antiknock additive, which used to be an important component in gasoline, should be replaced by unleaded antiknock additive. Methylcyclopentadienyl manganese tricarbonyl (MMT), as one of the alternate antiknock additives, has the advantage of low cost, improving the octane number and combustion efficiency of gasoline as well as reducing emission pollution.¹ The nature resource of methylcyclopentadienes (MCPD), the precursor of MMT, is extremely limited, and it is also difficult to obtain practical yield from the crack of petroleum, coal and other natural materials. Contrarily, cyclopentadiene (CPD) is a more abundant product, thus many researchers have endeavored to produce MCPD from the methylation of CPD.

In the earlier years, the synthesis of MCPD is through the following procedure: CPD reacts first with alkali metal sodium, and the formed cyclopentadienyl sodium then reacts with methylhalides to produce MCPD.^{2,3} This method has been used for producing commercial MCPD⁴ with the advantages of high yield (76–85%) and relative simple post-treatment procedure. However, it must be carried out in liquid ammonia, concerns the expensive reactants and easily generates excess dimethyl cyclopentadiene (DMCPD). Yoshida et al.^{5–7} develop a vapor-phase reaction of CPD with methanol in the presence of a catalyst such as an alkaline earth metal oxide, alkali metal oxide and alkali metal ion exchanged zeolites. In comparison to

the traditional way, replacing liquid alkali with solid base shows great advantages. The solid base catalyst can be easily separated from the products, and can be regenerated and reused. It is an environmentally benign process. However, commercial solid bases, especially for solid strong bases usually have small specific surface area, which is disadvantageous for the applications.⁸ Thus, it is very desirable to develop alternative methods to produce abundantly porous solid strong base with high specific surface area in a controllable manner.⁹ The sol–gel technique is one of most used methods to generate high specific surface area, and various solid bases have been prepared via this method.^{10–14} The chemical vapor deposition and reactive ballistic deposition approaches are also employed to generate high-specific-surface-area MgO.^{15,16} Exotemplating pathways are attracting considerable attention due to their simplicity.⁹ Several porous materials, such as porous silica,¹⁷ carbon,^{18–20} filter paper,²¹ diatoms,²² and CMK-3 carbon^{23,24} have been used as exotemplates to synthesize nanoporous MgO with higher specific surface area and wide pore size distributions (PSDs). The resulting materials serve as negative replicas of exotemplates.

Compared with man-made template materials, the natural plant materials are renewable, cheap and diverse, with structural and compositional hierarchical order.²⁵ In our previous work, natural plant materials such as cotton fiber and pine-wood were used as exotemplates to prepare biomorphic MgO particles.^{26–28} These materials possessed a nanocrystalline assembled mesoporous structure and exhibited high specific surface area and higher catalytic performance in CPD methylation.²⁹ Nevertheless, these biomorphic MgO materials are fragile, should be shaped into granules, spheres or extrudates prior to use as catalysts in practical processes.³⁰ Recently, we developed an *in situ* transformation technique to

^a Key Laboratory of Mesoscopic Chemistry of the Ministry of Education, School of Chemistry and Chemical Engineering, Nanjing University, Nanjing, 210093, China. E-mail: ychun@nju.edu.cn

prepare shaped MgO/carbon material. This MgO/carbon material presents the appearance of rice-grains, displays high specific surface area, and exhibits higher catalytic performance than MgO in the vapor-phase reaction of CPD with methanol.³¹ More importantly, it exhibits considerable mechanical strength due to the existence of carbon matrix, and can be directly used as catalyst. However, due to relative weaker basicity of MgO, the conversion of CPD on MgO/carbon materials is still unsatisfied. Moreover, the presence of black carbon affects the catalytic behavior of MgO in the methylation of cyclopentadiene, and the activity of catalyst decreases dramatically upon calcining in air to remove carbon. It is still a challenge to regenerate this carbon supported catalyst. In the present work, stronger basic CaO/carbon material has been prepared via *in situ* transformation approach. The resulting shaped CaO/carbon materials exhibited higher catalytic performance than MgO/carbon and CaO prepared by directly calcining CaO precursor. Moreover, we developed an effective route to regenerate the deactivated catalysts by steam or CO₂ treatment.

Experimental

Catalyst preparation

Biomorphic CaO/carbon materials were prepared via *in situ* transformation using calcium acetate monohydrate (Ca(Ac)₂·H₂O) (Beijing Chemical Reagent, China, ≥99.0%) as CaO precursor and rice grains purchased from a supermarket in Nanjing, China, as template and carbon precursor.³¹ Typically, a certain amount of Ca(Ac)₂·H₂O were dissolved into 10 ml of distilled water in a 50 ml beaker, and 20 g of rice grains, pre-washed with distilled water four times, was added to the solution and covered with a watch glass. The mixture was boiled in water bath until the solution was almost completely absorbed by the rice, usually between 40 and 90 minutes according to the dosage of Ca(Ac)₂·H₂O. The resulting cooked rice-like mixture was dried at 333K for ca.6~12 hours according to the dosage of Ca(Ac)₂·H₂O, and then calcined at 973 K in N₂ (80 mL/min) for 3 h. The resulting materials were denoted CaO(C)-x, where x indicates the mass ratio of Ca(Ac)₂·H₂O and rice grains.

For comparison, the *in situ* transformation route was used to prepare reference carbon from rice grains and reference MgO/carbon material from rice grains and magnesium acetate tetrahydrate, which were denoted C(rice) and MgO(C)-R, respectively. The sample CaO(R) was also used as a reference derived from directly calcining calcium acetate monohydrate at 973 K in air (1.5L/min).

Characterization

X-ray diffraction (XRD) patterns of samples were recorded on a Rigaku, D/max-RA diffractometer with Cu K α radiation in the 2 θ range from 5 to 90°. N₂ adsorption isotherms were measured using a Micromeritics ASAP 2020 system at 77 K. Sample was evacuated at 623 K for 4 h prior to testing. Specific surface area was determined using the Brunauer-Emmett-

Teller (BET) equation with adsorption branches in the relative pressure range from 0.04 to 0.2. Scanning electron microscopy (SEM) investigations were carried out on a Hitachi S-4800 field-emission instrument at an accelerating voltage of 10 kV. The elements and species on the surface were detected by X-ray photoelectron spectroscopy (XPS, PHI-5000, Japan). Base pressure in the analysis chamber was maintained in the range of 6.7×10⁻⁸ Pa. All samples were calcined at 973 K in the flowing of N₂ before adhering on double-sided tape on a sample rod, and then placed in the analysis position. The C 1s peak of CaCO₃ (289.6 eV) was used for the calibration of binding energies. When the carbonate peak was not observed, the C 1s peak of adventitious carbon (284.6 eV) was then used. The acidic-basic property of samples was determined by catalytic decomposition of isopropanol, which was measured in a conventional flow reactor at atmospheric pressure.³² The catalyst (50 mg) was activated at 973 K in the flow of N₂ (30 mL/min) for 1h and then cooled to the reaction temperature. The reactant isopropanol (Nanjing Chemical Reagent, China, ≥ 99.7%) was introduced using a syringe pump with the space velocity of 1.9 h⁻¹ in the flow of N₂ (20 mL/min). The reaction mixture was analyzed by on-line gas chromatography with a flame ionization detector (FID). The yield in this reaction were defined as Y_i= moles of product *i* formed per mole of isopropanol in the feed.

Catalytic testing

The vapor-phase methylation of cyclopentadiene (CPD) with methanol was carried out in a conventional flow reactor at atmospheric pressure.^{31,33} The catalyst (50 mg) was thermally activated at 973 K for 1 h in N₂ (30 mL/min) and cooled to the reaction temperature. CPD was obtained by thermal-depolymerization of dicyclopentadiene (Aldrich) at 873 K, and the reactants CPD and methanol (Nanjing Chemical Reagent, China, ≥99.7%) were introduced using syringe pumps with a molar ratio of 3.3 (space velocity of 3 h⁻¹) in the flow of N₂ (20 mL/min). The reaction was carried out in two modes: (1) the reaction was performed at different temperatures with the same reaction time of 10 min, for studying the effect of temperature on the catalytic activity and (2) the reaction was performed at different times with the same reaction temperature, for comparing the deactivation rate of different catalysts. The reaction mixture was analyzed by on-line GC. In order to study the regeneration of the deactivated catalyst, the spent CaO(C) was treated at 1023 K for 1 h in various atmospheres, and then cooled to the reaction temperature for further reaction. Conversion in this reaction was defined as C_r= moles of substrate reacted per mole of CPD in the feed, yield was defined as Y_i= moles of product *i* formed per mole of CPD in the feed, and selectivity was defined as S_i= moles of product *i* formed per mole of CPD reacted.

Results and discussion

Preparation of biomorphic CaO(C)

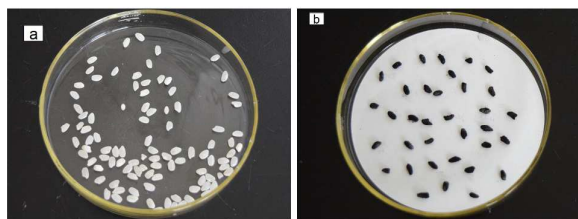


Fig. 1 Photographs of (a) raw rice grains and (b) CaO(C)-0.25 samples.

Rice grains have a spindle appearance, with a ca. 2-mm diameter and 5-mm length that varies with growing location and variety. The calcium acetate is poorly dispersed on the surface of raw rice grains by mechanical mixing or impregnation. However, calcium acetate is well dispersed on the swollen cooked rice grains that have absorbed water during the hydrothermal treatment. Black spindle CaO(C) particles were obtained by calcining these calcium acetate/cooked rice grains in nitrogen and are shown in Fig. 1. These CaO(C) particles display the spindle appearance of rice grains with a smaller size. The carbonaceous species that derived from the pyrolysis of rice grains provide a matrix with considerable mechanical strength. Therefore, these biomorphic CaO(C) particles can be directly applied in catalytic reaction without additional shaping.

Table 1 summarizes the preparation conditions. CaO content in CaO(C) samples varies from 10% to 47%, according to the dosage ratio of monohydrate calcium acetate and rice. However, it is difficult to disperse all the calcium salt when the dosage ratio exceeds 0.25, and thus some inhomogeneous particles can be distinguished from the rice-like particles in sample with high CaO content, especially for CaO(C)-1.0.

Characterizations of biomorphic CaO(C)

Fig. 2 shows wide-angle XRD patterns for the prepared CaO(C) samples and the effect of storage in air. As shown in Fig. 2(A), most of diffraction peaks in CaO(C) can be readily assigned to

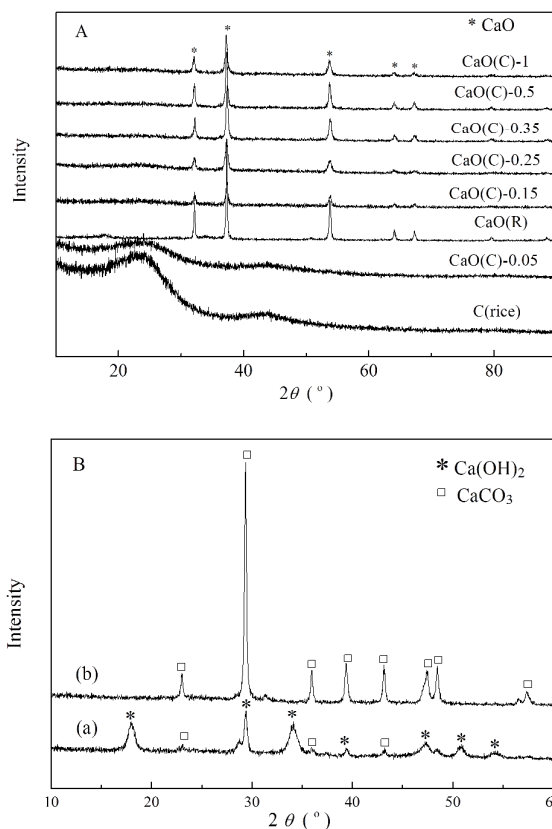


Fig. 2 XRD patterns of (A) biomorphic CaO(C) samples and (B) biomorphic CaO(C)-0.5 stored in air for 7 days (a) and 50 days (b).

the phase of CaO (JCPDS card number 37-1497), indicating that calcium acetate was converted into homogeneous CaO. Calculation using the Scherrer equation indicates these CaO particles have an average size between 30 and 40 nm (see Table 1), smaller than CaO(R) particles (69 nm) and commercial CaO particles (51 nm). As shown in Fig. 2(B), the CaO characteristic peaks are disappeared during the storage,

Table 1 Preparation conditions and texture parameters of biomorphic CaO(C) samples

Sample	Precursor mass (g)		CaO content (%)	Crystallinesize (nm, XRD)	A_{BET}^a (m^2/g)
	Ca(Ac) ₂ ·H ₂ O	Rice particle			
CaO(C)-0.05	1	20	10	---	46
CaO(C)-0.15	3	20	24	30	86
CaO(C)-0.25	5	20	36	34	107
CaO(C)-0.35	7	20	38	34	110
CaO(C)-0.5	10	20	41	34	151
CaO(C)-1	10	10	47	40	64
C(rice)	0	20	0	---	276
CaO(R)	10	0	100	69	15

^aSpecific surface area calculated using BET theory.

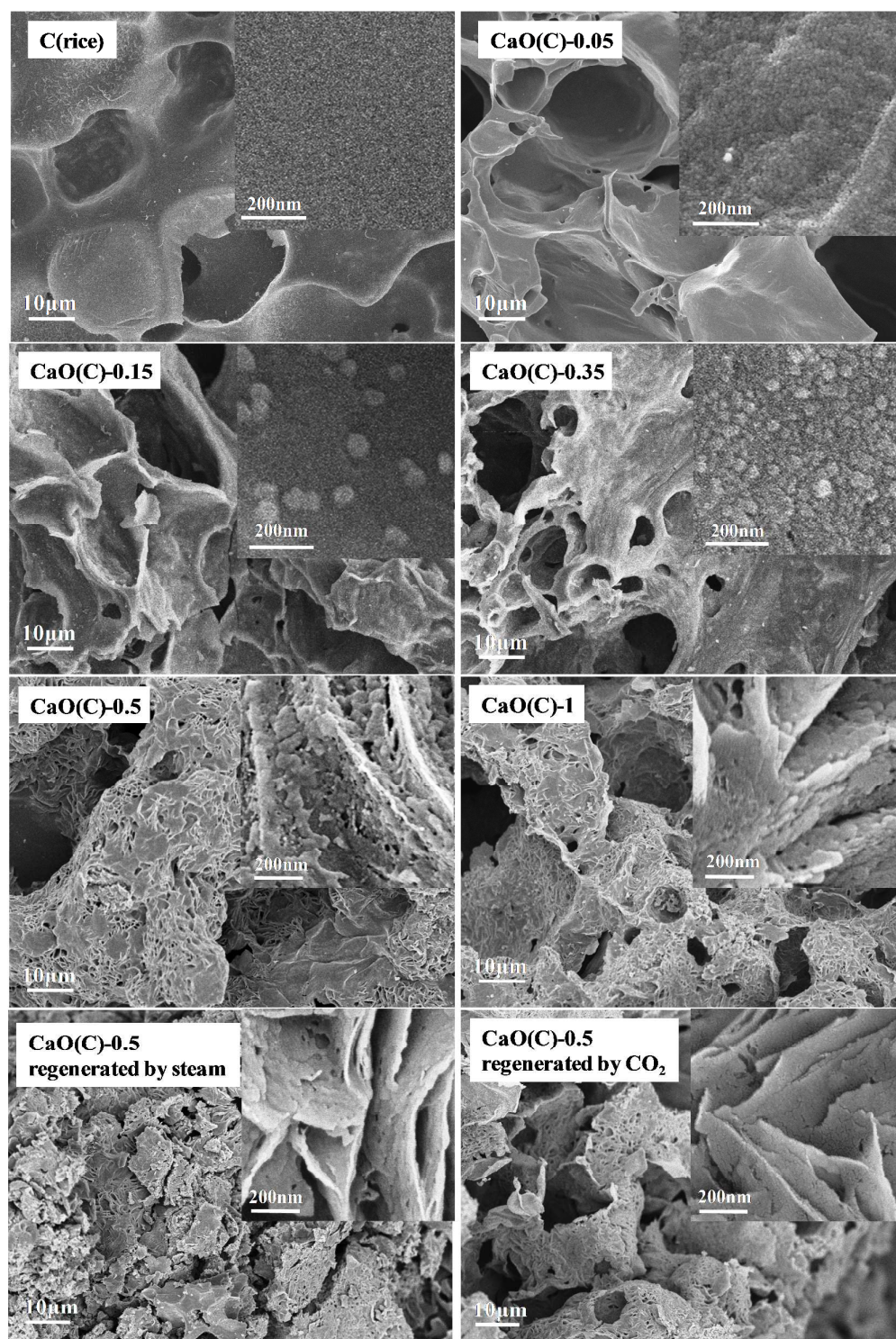


Fig. 3 SEM images of biomorphic CaO(C) and C(rice) samples.

indicating CaO is unstable during the storage of CaO(C). Nevertheless, both the products Ca(OH)_2 and CaCO_3 can be readily converted to CaO after calcining at 973 K in flowing of N_2 . It is worthy to note that Ca(OH)_2 and CaCO_3 are dominant

on CaO(C)-0.5 for one-week and 50-days storage, respectively, indicating that the CaO(C) sample is most possibly converted to Ca(OH)_2 first, and then slowly converted to CaCO_3 .

The BET specific surface areas of samples are listed in Table 1. CaO(R), which was prepared by directly calcining $\text{Ca}(\text{Ac})_2 \cdot \text{H}_2\text{O}$, shows a small specific surface area of $15 \text{ m}^2/\text{g}$. The biomorphic CaO(C) materials display the specific surface area ranged from 46 to $151 \text{ m}^2/\text{g}$, which is much higher than CaO(R). Similar to our previous result on $\text{MgO}(\text{C})$,³¹ the BET specific surface area increases almost monotonously with the dosage of CaO precursor, and CaO(C)-0.5 shows the highest specific surface area. Due to the blocking effect of excessive CaO, the specific surface area decreased apparently when the mass ratio of $\text{Ca}(\text{Ac})_2 \cdot \text{H}_2\text{O}$ and rice grains reaches 1.

Fig. 3 shows SEM images of biomorphic CaO(C) and C(rice). Generally, plenty of crater-like holes are observed on the SEM images of all the samples. These crater-like holes are in micrometer scale, and derived most possibly from the escape of water vapor or other gases during the calcination. Detailed observation can find that the hole wall on biomorphic CaO(C) and C(rice) is different. The hole wall on C(rice) is relatively flat, with some villiform species in nanometer scale on the surfaces. Similar to C(rice), a flat hole wall is observed on CaO(C)-0.05, indicating that CaO is well dispersed on the surfaces of carbon. With the increase of mass ratio of $\text{Ca}(\text{Ac})_2 \cdot \text{H}_2\text{O}$ and rice grains, a lot of spherical nano-particles are formed on the hole wall. These nanocrystals are inserted in the carbon framework more or less, and have a diameter around 30 nm, in coincidence with the CaO particle size calculated based on XRD patterns. A kind of laminated surface structure is formed when mass ratio of $\text{Ca}(\text{Ac})_2 \cdot \text{H}_2\text{O}$ and rice grains reaches 0.5. This dramatic change of the hole wall derives from the stacking of excessive CaO on the surfaces of sample. The high magnification SEM image shows that the

laminated structure has a layer thickness of a few tens of nanometers, and is more compact at higher CaO content. It seems to suggest that surface CaO on biomorphic CaO(C) samples grows up from dispersed little particles to nanocrystals, and then to lamination with the increase of usage of $\text{Ca}(\text{Ac})_2 \cdot \text{H}_2\text{O}$.

Fig. 4 shows the X-ray photoelectron spectra for the Ca 2p, C 1s and O 1s core levels of CaO(R), biomorphic CaO(C)-0.05 and CaO(C)-0.5 samples. The Ca 2p exhibits a doublet with a separation of 3.5 eV, $2p_{3/2}$ and $2p_{1/2}$ components. The BE of two Ca $2p_{3/2}$ components at 347–347.1 eV and 346.2 eV arise from CaCO_3 and $\text{Ca}(\text{OH})_2$ species, respectively.^{34,35} Therefore, the outermost surface layers of CaO in these samples is extensively carbonated and hydrated. Due to the superbacidity, surface CaO in CaO(C) and CaO(R) catalysts can rapidly react with H_2O and CO_2 in the air, and forming hydroxide and carbonate salts.³⁶ The peak at 289.6 eV is pronounced in C 1s spectra of CaO(R) and biomorphic CaO(C)-0.5, giving the further evidence on the formation of carbonate salts (it was used as a reference for the rest of the core levels³⁵). Another intense peak at 284.6 eV was assigned to carbon supporter and common organic pollutants. A third peak at 286.2–286.8 eV is also visible after deconvolution of the C 1s level, which due to C present in carbonyl, alcohols or ether groups.³⁷

All of the samples possess broad O 1s spectra at 531.2–531.5 eV, which is assigned to the contributions of $\text{Ca}(\text{OH})_2$ and CaCO_3 .³⁵ The deconvolution of this broad peak is difficult since the O 1s peaks arising from OH^- and CO_3^{2-} groups are separated by less than 0.5 eV. It can be found that the binding energies of the O 1s in biomorphic CaO(C)-0.5 is lower than that in CaO(C)-0.05. However, it is unreasonable to evaluate

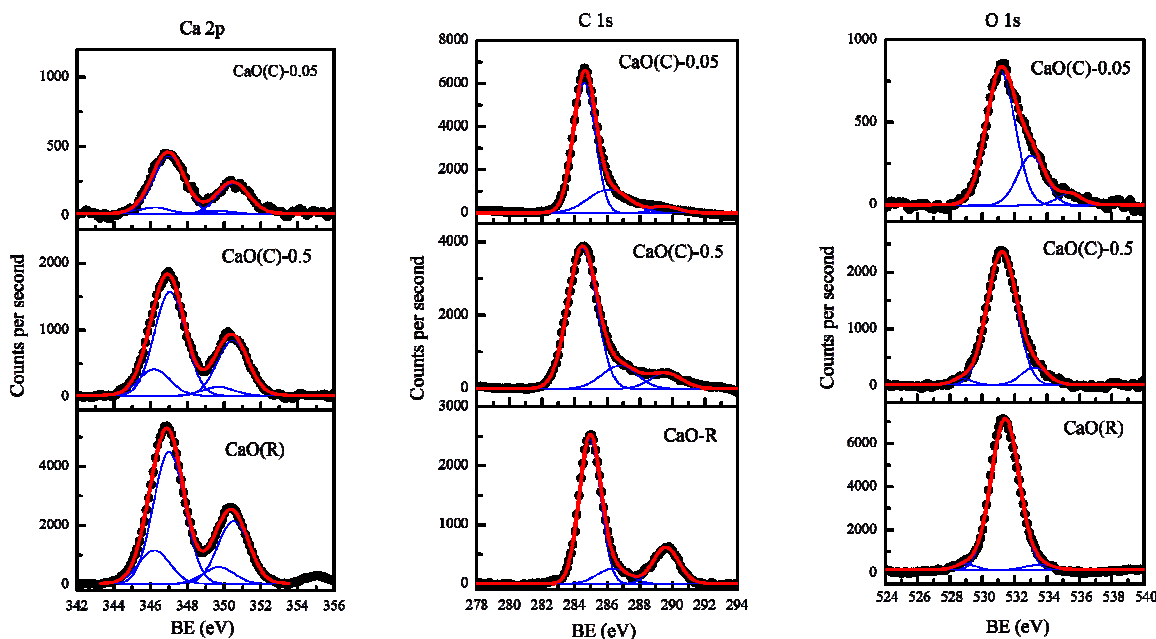


Fig. 4 Ca 2p, C 1s and O 1s core levels of CaO(R), biomorphic CaO(C)-0.5 and CaO(C)-0.05 samples.

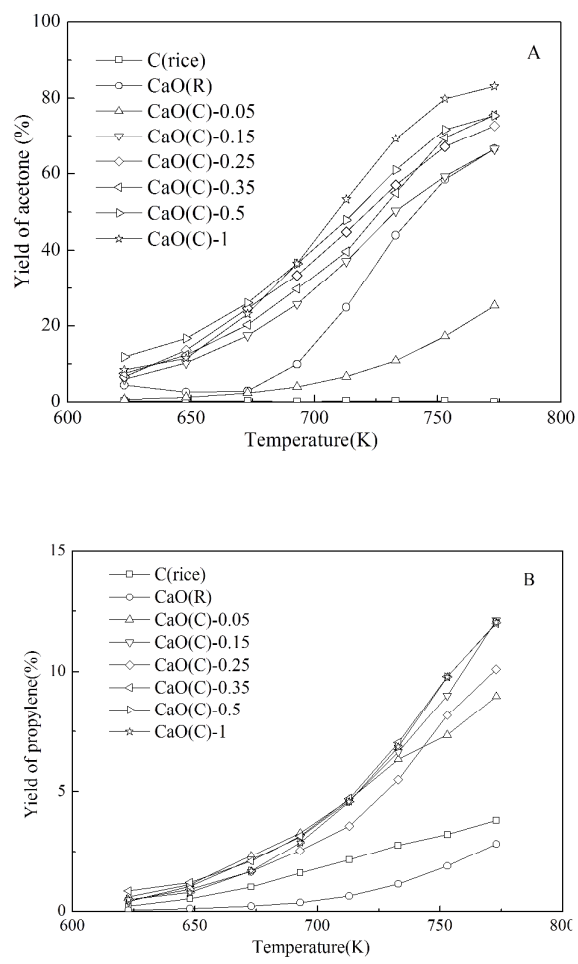


Fig.5 (A) Yield of acetone and (B) yield of propylene on biomorphic CaO(C) samples. (space velocity= 0.9 h^{-1} , $p=101\text{kPa}$).

the basicity of samples by directly comparing the BE of this peak, since $\text{Ca}(\text{OH})_2$ and CaCO_3 arise from the reaction of CaO with H_2O and CO_2 in the air. Contrarily, a small peak at 528.8–529.0 eV in CaO(C)-0.5 and CaO(R), which arises from the CaO framework O^{2-} ,^{35,38} is more close to the actual state of the basic sites. It is clearly seen that the BE of this small peak in CaO(C)-0.5 is similar to CaO(R), indicating the existence of CaO in CaO(C)-0.5 with the basicity similar to pure CaO. Detailed observation can find the width of O 1s peak in biomorphic CaO(C), especially for CaO(C)-0.05 is larger than that in CaO(R), and some peaks at higher BE (533.0–535.6 eV) are also visible after deconvolution of O 1s level, which may arise from the oxygen-containing functional groups on carbon supporter.³⁹ These components at higher BE have a certain effect on the basicity of samples, especially for CaO(C)-0.05.

The acidic-basic properties of the biomorphic CaO(C) samples were evaluated by catalytic decomposition of isopropanol. It is well known that propylene and water are

generated on the acidic sites while acetone and hydrogen are formed on basic sites in this probe catalytic reaction.⁴⁰ As shown in Fig. 5, yield of acetone on C(rice) is close to zero, indicating that the basicity of carbon is very weak. The sample CaO(R) shows weak basic catalytic performance due to its small specific surface area ($15 \text{ m}^2/\text{g}$). Actually, pure CaO derived from calcination of inorganic calcium precursors,^{41,42} sol-gel combustion synthesis,^{43–45} precipitated calcium carbonate⁴⁶ or other methods^{47–52} usually shows small specific surface area. The yield of acetone on CaO(C)-0.05 is lower than that on CaO(R), indicating the basicity of CaO(C)-0.05 is weaker than CaO(R). However, the yield of acetone increases with the increase of the mass ratio of calcium acetate monohydrate and rice grains. When the mass ratio reaches 0.15 or higher, the resulting CaO(C) samples exhibit stronger basicity than CaO(R).

Biomorphic CaO(C)-0.05 shows the basicity apparently lower than other biomorphic CaO(C) samples. One of the possible reason is that this sample has lowest CaO content. Moreover, some oxygen-containing functional groups are existed on the surfaces of carbon support, which would result in surface acidity.⁵³ Zu et al.⁵⁴ have reported two types of “CaO” phases in the nanoporous carbon-supported CaO catalysts: The type-I phase has strong interaction with surface oxygen-containing functional groups of carbon supports and having weaker basicity and lower activity; The type-II phase exhibits a relatively weak interaction with supports, showing stronger basicity and higher activity. Similar to these catalysts, partial of CaO in biomorphic CaO(C) samples would have strong interaction with the oxygen-containing functional groups in carbon support, and may have a certain effect on the basicity. For most of samples, this effect is not pronounced since the content of the oxygen-containing functional groups is low for carbon pyrolyzed at 973K.⁵³ However, it cannot be ignored for CaO(C)-0.05 due to lower CaO content, and thus would decrease the basicity of CaO(C)-0.05 apparently.

Catalytic behavior of biomorphic CaO(C)

The catalytic behavior of biomorphic CaO(C) samples in the methylation of CPD with methanol is shown in Fig.6-7. In this reaction, CPD and methanol were dehydrogenated on the strong basic sites first, and the resulting cyclopentadienyl anion and formaldehyde were further converted to the target products methylcyclopentadienes (MCPD).³³ The main by-products dimethylcyclopentadienes (DMCPD) and cyclopentene are produced by deep methylation of MCPD and hydrogenation of CPD, respectively. In addition, some light compounds, e.g. CO , CH_4 , CO_2 and H_2 , can also be produced through decomposition of methanol on basic sites.

Fig.6 depicts the catalytic behavior of various catalysts in the methylation of CPD with methanol. C(rice) hardly has any catalytic activity on generating MCPD due to its inert surface. The conversion of CPD and yield of MCPD on CaO(R) are very small, which should be ascribed to its small specific surface area. Biomorphic CaO(C)-0.5 exhibits a catalytic performance clearly superior to C(rice) and CaO(R), and the yield of MCPD is over 15% at a reaction temperature between 673 and 773 K.

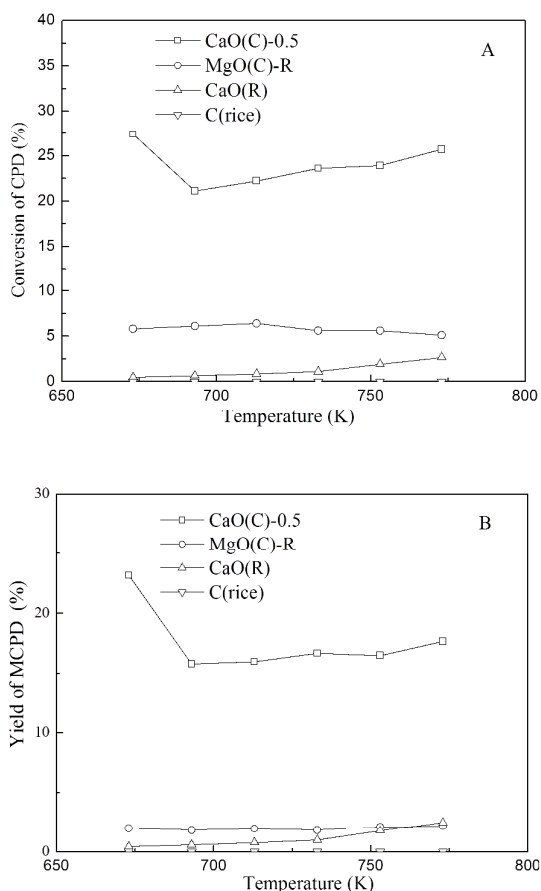


Fig.6 (A) Conversion of CPD and (B) yield of MCPD with methanol/CPD ratio of 3.3 (space velocity = 2.5 h^{-1}) as functions of temperature on various samples ($p = 101 \text{ kPa}$).

The catalytic performance of CaO(C)-0.5 is also superior to that of MgO(C)-R, which has a similar mole loading amount of base and was prepared via same *in situ* transformation. The conversion on Ca(C)-0.5 is nearly four times as high as on MgO(C)-R, and the yield of MCPD is eight times as high as on MgO(C)-R. It is well known that MgO is a strong base while CaO degassed at 973 K exhibits superbasicity. We have found that introduction of superbasic sites is an important factor to improve catalytic performance of MgO in CPD methylation, which can be ascribed to acceleration of dehydrogenization of CPD and methanol.³³ Therefore, the superbasicity of CaO should be responsible for better catalytic performance of CaO(C).

As shown in Fig. 7, the dosage of rice grains has an apparent effect on the conversion of CPD. The catalytic performance is enhanced with the increase of the mass ratio of $\text{Ca}(\text{Ac})_2 \cdot \text{H}_2\text{O}$ and rice grains. CaO(C)-0.5 exhibits the best catalytic performance, with 27% conversion and 23% yield for MCPD at 673 K. The catalytic performance of these CaO(C) samples is coincident with their basicity. This is evident in the

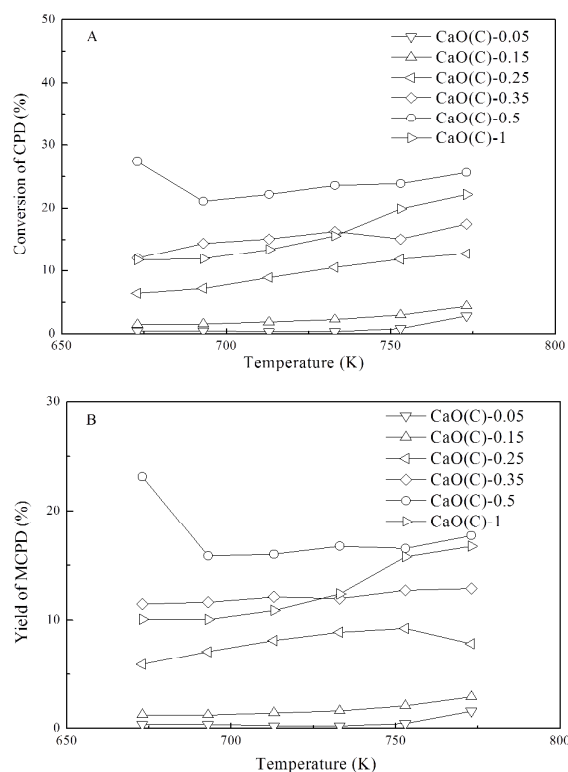


Fig.7 (A) Conversion of CPD and (B) yield of MCPD with methanol/CPD ratio of 3.3 (space velocity = 2.5 h^{-1}) as functions of temperature on biomorphic CaO(C) samples ($p = 101 \text{ kPa}$).

catalytic decomposition of isopropanol. It is worth mentioning that dispersion degree of CaO on carbon has a great effect on the catalytic performance. Dispersed CaO nanocrystals on carbon (i.e. CaO(C)-0.35, CaO(C)-0.5) exhibit high catalytic activity, while aggregated CaO (i.e. CaO(R)) show hardly any catalytic activity in this temperature range. This can be attributed to the difference of the specific surface area. CaO(R) shows a specific surface area much lower than biomorphic CaO(C) samples (see Table 1). CaO(C)-0.05 shows poor catalytic activity in CPD methylation, although CaO was well dispersed on this sample. Compared to other CaO(C) samples, CaO(C)-0.05 has lowest CaO content and specific surface area, which are disadvantaged for the catalytic activity. On the other hand, the basicity of CaO(C)-0.05 was decreased by the oxygen-containing functional groups in carbon support, which would decrease the catalytic activity also. CaO(C)-1 shows a catalytic performance inferior to CaO(C)-0.5, one of the possible reasons is that CaO(C)-1 has a specific surface area lower than CaO(C)-0.5. Moreover, although the CaO content on CaO(C)-1 is higher than CaO(C)-0.5, many of them are aggregated into

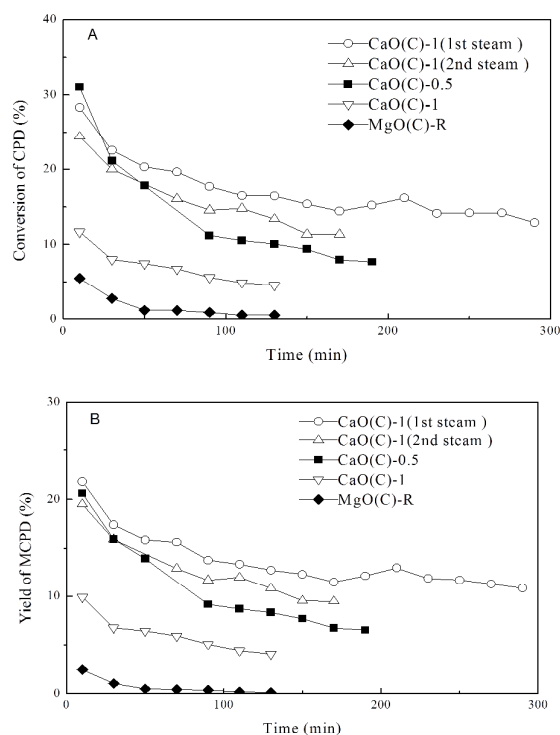


Fig.8 (A) Conversion of CPD and (B) yield of MCPD methanol/CPD ratio of 3.3 (space velocity = 2.5 h⁻¹) as functions of time at 673K on biomorphic CaO(C) and MgO(C) samples (p = 101 kPa). First steam and 2nd steam indicated the results on regenerated CaO(C)-1 sample by streaming once and twice, respectively.

CaO laminated structure, which is not as active as dispersed CaO nanocrystals on carbon in CPD methylation.

Deactivation and regeneration of biomorphic CaO(C)

Fig.8 illustrates the time-on-stream behavior of biomorphic CaO(C) and MgO(C) catalysts during the methylation of CPD at 673 K. The activities of CaO(C)-0.5 and MgO(C)-R decay gradually along the catalytic test. It can be found that the initial decaying rate on CaO(C)-0.5 is a little faster than MgO(C)-R. However, the conversion of CPD and yield of MCPD

Table 3 The catalytic performance of spent CaO(C)-0.5 upon activation in various atmospheres

Atmosphere	C _{CPD} ^a (%)	Y _{MCPD} ^b (%)	S _{MCPD} ^c (%)
--	0.1	0.03	38
air	0	0	0
N ₂	6.4	5.1	79
H ₂	8.9	4.9	55
CO ₂	33	26	79
H ₂ O	34	27	81

^aConversion of cyclopentadiene. ^bYield of methylcyclopentadiene. ^cSelectivity of methylcyclopentadiene.

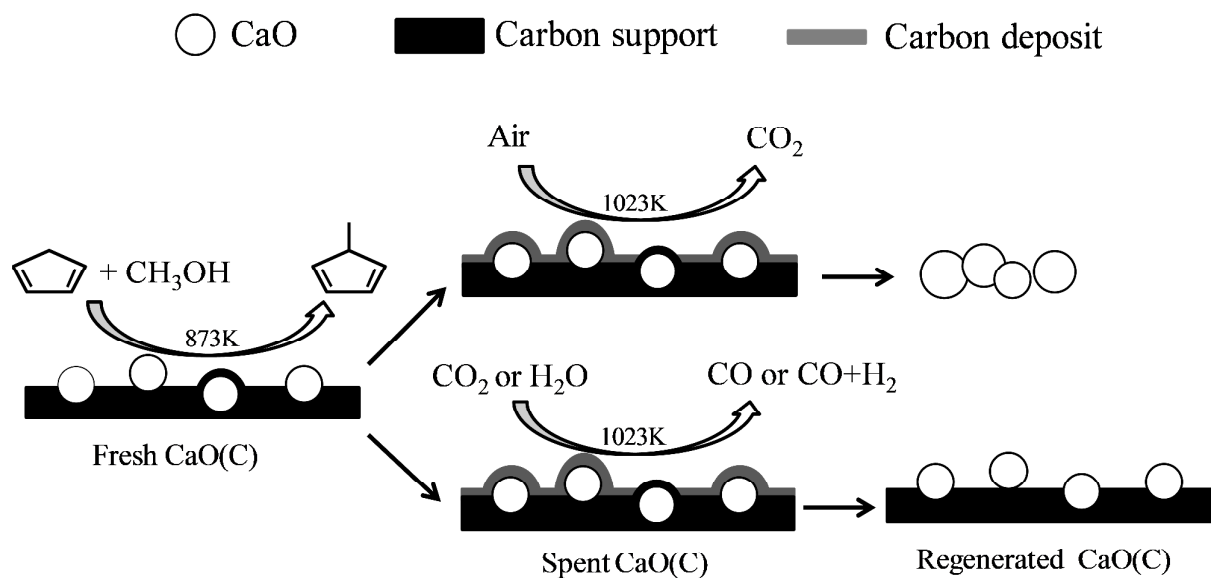
on CaO(C)-0.5 after 130 min run are 7.7% and 6.5%, respectively, still higher than the initial values on MgO(C)-R. The deactivation of solid base catalyst in CPD methylation can be ascribed to the effect of carbon deposits.³³ However, we have found that the presence of black carbon promotes the catalytic performance of MgO(C) in the methylation of CPD, and the activity of catalyst declined dramatically upon calcining in air to remove carbon.³¹ Thus conventional regeneration route, i.e. removing carbon by calcining in the air, is unsuitable for this kind of deactivated catalysts.

In order to search for an effective regenerating method, CaO(C)-0.5 catalyst was firstly deactivated by reaction at 873 K, and then underwent the calcination at 1023 K with different atmospheres. The catalytic performance of regenerated sample was detected by the methylation of CPD at 673 K, and the reaction results are listed in Table 3. Both the conversion and yield of MCPD are near 0 when deactivated CaO(C)-0.5 is calcined in the air. It is not surprised since the carbon is removed off and the resulting CaO shows poor catalytic performance at this temperature. Activation in flowing of N₂ or H₂ can partially recover the catalytic activity. The most possible reason is that the carbonaceous species covered on the active sites are partially removed or further carbonized. Nevertheless, the yields of MCPD on these regenerated catalysts are ca. 5%, far lower than 21% on fresh catalyst. It is delighted to find that the spent CaO(C)-0.5 exhibits good

Table 4 The catalytic performance of CaO(C)-0.5 during the deactivation and steam treatment

Catalyst	In CPD methylation		In isopropanol decomposition		Δm (mg) ^e
	C _{CPD} (%) ^a	Y _{MCPD} (%) ^b	Y _A (%) ^c	Y _P (%) ^d	
Fresh	23	19	29	3	0
Deactivated	0.1	0.03	0.05	0	+5.9
Regenerated ^f	35	29	45	5	-12.8

^aConversion of cyclopentadiene. ^bYield of methylcyclopentadiene; ^cYield of acetone. ^dYield of propylene. ^emass change with fresh catalyst. ^fRegeneration was performed by steam treatment at 1023 K.



Scheme 1. Schematic representation for the regeneration of CaO(C) by steam, CO₂ and air treatments.

catalytic performance in CPD methylation if activation in flowing of steam or CO₂ at 1023 K. The conversion of CPD and the yield of MCPD on both regenerated samples can reach 33% and 26%, respectively, which are even higher than those on fresh CaO(C)-0.5.

In order to reveal the change of surface property during the deactivation and steam treatment, catalytic decomposition of isopropanol was employed to evaluate the acidic-basic properties of fresh, deactivated and regenerated CaO(C)-0.5, and the result is listed in Table 4. It can be found that the yield of acetone decreased from 29% to 0.05% when fresh CaO(C)-0.5 was deactivated in CPD methylation, indicating that the basicity of CaO(C)-0.5 decreased dramatically during the deactivation. After steam treatment, 45% of yield of acetone was detected on this catalyst, which is even higher than the fresh one. Obviously, the regenerated catalyst exhibits stronger basicity. This change of basicity on CaO(C)-0.5 is coincident with that of the catalytic performance in CPD methylation during deactivation and regeneration. Table 4 also shows the change of mass on CaO(C)-0.5 after deactivation and regeneration. It can be found that the mass of catalyst increased by 5.9 mg during deactivation, which is derived from carbon deposit. After steam treatment, the mass of catalyst decreased by 12.8 mg, which is derived from the reaction of water with carbon. The value of mass loss during regeneration exceeds that of mass increment during deactivation, which indicated that steam treatment removed not only the carbon deposit but also part of the carbon support. Furthermore, the SEM images of CaO(C)-0.5 regenerated by steam (or by CO₂) treatment show the laminated surface structure, similar to

that of fresh CaO(C)-0.5 (Fig. 3). It indicates that the steam or CO₂ treatment has little effect on the appearance of CaO(C).

Scheme 1 depicts the possible mechanism for the regeneration of deactivated CaO(C) by CO₂ and steam. As discussed above, it is very important to selectively remove carbon deposit rather than carbon support, in order to recover the activity of the spent catalyst. The carbon deposit is on the surfaces of catalyst, while the carbon support locates mainly the inside of the catalyst. During the regeneration, the oxidative gas reacts with carbon deposit before reacting with carbon support, thus it is possible to realize selective remove of carbon deposit. However, the reaction of carbon with O₂ is too strong to control, and both the carbon deposit and carbon support are removed upon air treatment. Contrarily, the reactions of carbon with CO₂ or steam are more moderate, it is easy to realize this selective oxidation by controlling suitable reaction condition.

Fig. 8 also illustrates the time-on-stream behavior of regenerated CaO(C)-1 by steaming treatment. It clearly shows that the activity of CaO(C)-1 is improved after regenerating. The initial yield of MCPD on regenerated CaO(C)-1 is 22%, much higher than that on fresh one (ca. 10%). It is worth mentioning that the yield of MCPD on regenerated catalyst is ca. 12% after 250 min run, which is even higher than the initial yield on fresh catalyst. Since the CaO(C)-1 catalyst is prepared by *in situ* transformation, the carbons derived from the pyrolysis of rice grains mostly function as a matrix to disperse CaO nanocrystals. However, some of them may cover the surfaces of active sites and suppress the conversion of CPD. Therefore, the promotion of catalytic performance is most possibly ascribed to the removal of the carbon that covered

the active sites by steaming. Moreover, the twice regenerated CaO(C)-1 sample can still exhibit high catalytic performance, indicating the catalyst can be used repeatedly by steaming. It is very important for the industrial application.

Conclusions

Biomorphic CaO(C) materials with a uniformly spindly appearance can be synthesized via *in situ* transformation using rice grains as the template and carbon precursor. These CaO/carbon materials have high specific surface area, and exhibit catalytic performance for CPD methylation superior to MgO/carbon and CaO prepared by directly calcining CaO precursor. The spent catalyst can be regenerated by steam or CO₂ treatment.

The approach to prepare biomorphic CaO(C) is a simple and low-cost strategy. More importantly, this CaO(C) material can be directly used as a shaped catalyst and regenerated by simply stream or CO₂ treatment. It displays the potential for a high efficiency and low-cost solid base catalyst.

Acknowledgements

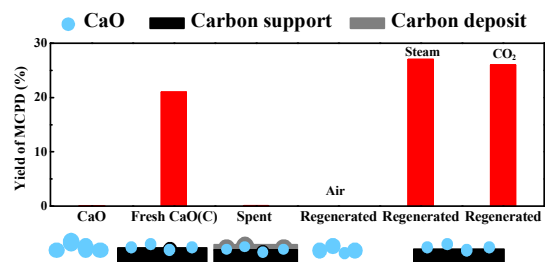
This work was supported by the National Natural Science Foundation of China (21273108).

Notes and references

- F. J. Wu, B.C. Berris and D.R. Bell, US Patent 4 946 975, to Ethyl Co., Ltd. 1990.
- S. Mclean and P. Haynes, *Tetrahedron.*, 1965, **21**, 2313-2327
- V.A.Mironov, E.V. Sobolev and A.N. Elizavova, *Tetrahedron.*, 1963, **19**, 1939-1958.
- S.J. Rajan, US Patent 4 547 603, to Ethyl Co., Ltd., 1982
- Z. Yoshida, S. Kato, Y. Amemiya and K. Yanai, US Patent 4 567 308, to Asahi Chemical Co., Ltd. 1985.
- Z. Yoshida, S. Kato and Y. Amemiya, EP Patent 0 256 228, to Asahi Chemical Co.,Ltd. 1987.
- Z. Yoshida, S. Kato and Y. Amemiya, US Patent 4814532, to Asahi Chemical Co., Ltd. 1989.
- K. T. Ranjit and K. J. Klabunde, *Chem. Mater.*, 2005, **17**, 65-73.
- W.C. Li, A.H. Lu, C. Weidenthaler and F. Schuth, *Chem. Mater.*, 2004, **16**, 5676-5681.
- C. Zhang, W. Xiang, H. Luo, H. Liu, X. Liang, X. Ma, L. Pei, Z. Chen, J. Li, H. Gao and L. Ma, *J. Alloy. Compd.*, 2014, **602**, 221-227
- R.M. Richards, A.M. Volodin, A.F. Bedilo and K.J. Klabunde, *Phys. Chem. Chem. Phys.*, 2003, **5**, 4299-4305.
- M.E. Martin, R.M. Narske and K.J. Klabunde, *Micropor. Mesopor. Mater.*, 2005, **83**, 47-50.
- R. Richards, W. Li, S. Decker, C. Davidson, O. Koper, V. Zaikovski, A. Volodin, T. Rieker and K.J. Klabunde, *J. Am. Chem. Soc.*, 2000, **122**, 4921-4925.
- H. Jeon, D. J. Kim, S. J. Kim and J. H. Kim, *Fuel. Process. Technol.*, 2013, **116**, 325-331.
- E. Knozinger, K.H. Jacob, P. Hofmann and *J. Chem. Soc., Faraday Trans.*, 1, 1993, **89**, 1101-1107.
- E. Knozinger, O. Diwald and M. Sterrer, *J. Mol. Catal. A.*, 2000, **162**, 83-95.
- J. Lee, S. Han and T. Hyeon, *J. Mater. Chem.*, 2004, **14**, 478-486.
- F. Schuth, *Angew. Chem., Int. Ed.*, 2003, **42**, 3604-3622.
- R. Ryoo, S.H. Joo, M. Kruk and M. Jaroniec, *Adv. Mater.*, 2001, **13**, 677-681.
- M. Schwickardi, T. Johann, W. Schmidt and F. Schuth, *Chem. Mater.*, 2002, **14**, 3913-3919.
- A. N. Shigapov, G. W. Graham, R. W. McCabe and H. K. Plummer Jr., *Appl. Catal. A.*, 2001, **210**, 287-300.
- K. H. Sandhage, M. B. Dickerson, P. M. Huseman, M. A. Caranna, J. D. Clifton, T. A. Bull, T. J. Heibel, W. R. Overton and M. E. A. Schoenwaelder, *Adv. Mater.*, 2002, **14**, 429-433.
- J. Roggenbuck and M. Tiemann, *J. Am. Chem. Soc.*, 2005, **127**, 1096-1097.
- J. Roggenbuck, G. Koch and M. Tiemann, *Chem. Mater.*, 2006, **18**, 4151-4156.
- Z. Liu, T. Fan and D. Zhang, *J. Am. Ceram. Soc.*, 2006, **89**, 662-665.
- R. Q. Sun, X. Zhou, L. B. Sun, H. Wu, Y. Chun and Q. H. Xu, *Chem. J. Chin. Univ.*, 2007, **28**, 2333-2337.
- R.Q. Sun, L.B. Sun, Y. Chun, Q.H. Xu and H. Wu, *Micropor. Mesopor. Mater.*, 2008, **111**, 314-322.
- L. Ma, P. Jiang, R.Q. Sun, Y. Chun and Q.H. Xu, *Chin. J. Catal.*, 2009, **30** (7), 631-636.
- D.X. Lan, D. Lin, H.M. Zhao, L. Ma and Y. Chun, *Chin. J. Catal.*, 2011, **32** (7) 1214-1219.
- G. Chandrasekar, M. Hartmann and V. Murugesan, *J. Por. Mater.*, 2009, **16**, 175-183.
- L. Ma, X. Y. Zhang, D. Lin, Y. Chun and Q. H. Xu, *Appl. Catal. A.*, 2013, **460-461**, 26-35.
- R.Q. Sun, L.B. Sun, Y. Chun and Q.H. Xu, *Carbon.*, 2008, **46**, 1757-1764.
- D. X. Lan, L. Ma, Y. Chun, C. Wu, L. B. Sun and J. H. Zhu, *J. Catal.*, 2010, **275**, 257-269.
- S. Yan, M. Kim, S. Mohan, S.O. Salley and K.Y. S. Ng, *Appl. Catal. A*, 2010, **373**, 104-111.
- M. L. Granados, M.D. Z. Poves, D. M. Alonso, R. Mariscal, F. C. Galiste, R. Moreno-Tost, J. Santamari and J.L.G. Fierro, *Appl. Catal. B*, 2007, **73**, 317-326.
- S. Yan, H. Lu and B. Liang, *Energy Fuels*, 2008, **22**, 646-651.
- S. Biniak, G. Szymanski, J. Siedlewski and A. Swiatkowski, *Carbon*, 1997, **35**, 1799-1810.
- V. Dimitrov, *J. Solid State Chem.*, 2002, **163**, 100-112.
- G. G. Wildgoose, N. S. Lawrence, H. C. Leventis, L. Jiang, T. G. J. Jonesb and R. G. Compton, *J. Mater. Chem.*, 2005, **15**, 953-959.
- P. E. Hathaway and M. E. Davis, *J.Catal.*, 1989, **116** (1), 263-278.
- H. Lu, A. Khan and P. G. Smirniotis, *Ind. Eng. Chem. Res.*, 2008, **47**, 6216-6220.
- W. Q. Liu, N.W.Low, B. Feng, G.X.Wang and J.D.D.Costa, *Environ. Sci. Technol.*, 2010, **44**, 841-847.
- M. Broda, A.M. Kierzkowska and C.R. Müller, *ChemSusChem.*, 2012, **5**, 411-418.
- A. Akgornpeak, T.Witton, T. Mungcharoen and J. Limtrakul, *Chem. Eng., J.*, 2014, **237**, 189-198.
- H. R. Radfarnia and A. Sayari, *Chem. Eng. J.*, 2015, **262**, 913-920.
- H. Gupta and L. S. Fan, *Ind. Eng. Chem. Res.*, 2002, **41**, 4035-4042.
- X. D. Zhang, L. Z. Sun, L.Chen, X.P.Xie, B.F.Zhao, H.Y.Si and G.F.Meng, *J. Anal. Appl. Pyrolysis.*, 2014, **108**, 35-40.
- A. Antzara, E. Heracleous and A.A.Lemonidou, *Energy Procedia.*, 2014, **63**, 2160-2169.
- H. R. Radfarnia and M. C. Iliuta, *Chem. Eng. J.*, 2014, **109**, 212-219.
- H. Petitjean, J.M. Krafft, M. Che, H.Lauron-Pernot and G. Costentin, *J. Phys. Chem. C*, 2011, **115**, 751-756.

- 51 J. M. Valverde, P. E. Sanchez-Jimenez and L. A. Perez-Maqueda, *J. Phys. Chem. C*, 2015, **119**, 1623–1641.
- 52 R. Koirala, K. R. Gunugunuri, S. E. Pratsinis and P. G. Smirniotis, *J. Phys. Chem. C*, 2011, **115**, 24804–24812.
- 53 Y. Chun, G. Sheng, C. T. Chiou and B. Xing, *Environ. Sci. Technol.*, 2004, **38**, 4649–4655.
- 54 Y. Zu, G. Liu, Z. Wang, J. Shi, M. Zhang, W. Zhang and M. Jia, *Energy Fuels*, 2010, **24**, 3810–3816.

Table of Contents



Shaped CaO/carbon catalysts *prepared via in situ* transformation exhibit high activity and can be regenerated by steam or CO₂ treatment.